

# “Brill Transition” Shown by Green Material Poly(octamethylene carbonate)

Ti-Peng Zhao,<sup>†,‡</sup> Xiang-Kui Ren,<sup>§</sup> Wen-Xiang Zhu,<sup>†</sup> Yong-Ri Liang,<sup>||</sup> Chun-Cheng Li,<sup>†</sup> Yong-Feng Men,<sup>⊥</sup> Chen-Yang Liu,<sup>\*,†</sup> and Er-Qiang Chen<sup>\*,#</sup>

<sup>†</sup>Beijing National Laboratory for Molecular Sciences, CAS Key Laboratory of Engineering Plastics, Joint Laboratory of Polymer Science and Materials, Institute of Chemistry, The Chinese Academy of Sciences, Beijing 100190, People's Republic of China

<sup>‡</sup>University of Chinese Academy of Sciences, Beijing 100049, People's Republic of China

<sup>§</sup>School of Chemical Engineering and Technology, Tianjin University, Tianjin 300072, People's Republic of China

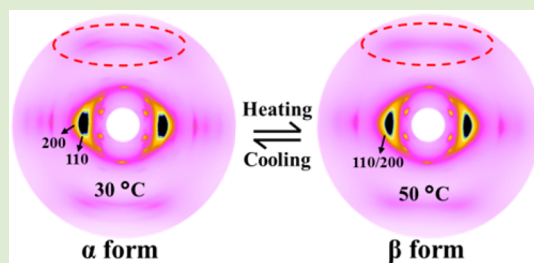
<sup>||</sup>College of Materials Science and Engineering, Beijing Institute of Petrochemical Technology, Beijing 102617, People's Republic of China

<sup>⊥</sup>State Key Laboratory of Polymer Physics and Chemistry, Changchun Institute of Applied Chemistry, Chinese Academy of Sciences, University of Chinese Academy of Sciences, Renmin Street 5625, 130022 Changchun, People's Republic of China

<sup>#</sup>Beijing National Laboratory for Molecular Sciences, Key Laboratory of Polymer Chemistry and Physics of the Ministry of Education, Center for Soft Matter Science and Engineering, College of Chemistry and Molecular Engineering, Peking University, Beijing 100871, People's Republic of China

## S Supporting Information

**ABSTRACT:** Poly(octamethylene carbonate) (POMC), as the eighth member of the newly developed biodegradable aliphatic polycarbonate family, demonstrates a reversible crystal–crystal transition, which is highly similar to Brill transition extensively studied in the nylon family. With the dipole–dipole interaction in POMC much weaker than the hydrogen bonding, POMC exhibits its “Brill transition” temperature at around 42 °C, much lower than nylons. The two crystalline structures of POMC at below and above the transition temperature can be identified. The transition of POMC is largely associated with the reversible conformation change of methylene sequences from trans-dominated at low temperatures to trans/gauche coexistence at high temperatures.



In recent years, biodegradable polymers are attracting increasing interest owing to their great potential to solve the problems of plastic pollution.<sup>1–4</sup> As an important class of biodegradable polymers, aliphatic polycarbonates (APCs) have excellent physical and chemical properties, biocompatibility, and nontoxicity. Particularly, they do not produce an acid compound after degradation.<sup>5–8</sup> Therefore, APCs can not only replace some nonbiodegradable materials used in packaging, agriculture, and so on but, more importantly, have great application potential in the areas of biomedicine and pharmaceuticals.<sup>9–11</sup> Recently, a series of high molecular weight (MW) APCs (-(CH<sub>2</sub>)<sub>m</sub>-O-CO-O-)<sub>n</sub>, *m* = 3–10) are successfully synthesized by using the novel TiO<sub>2</sub>/SiO<sub>2</sub>-based catalyst.<sup>11</sup> Thermal<sup>12</sup> and rheological<sup>13</sup> properties of high MW APCs were investigated. Similar to other aliphatic polyesters with regular chemical structure, APCs are semicrystalline.<sup>10,12</sup> Takahashi et al. have reported that poly(trimethylene carbonate) can form a triclinic structure after a long time crystallization at rather low temperatures.<sup>14</sup> Upon molecular dynamic (MD) simulation, chain packing schemes of other APCs with different *m* were suggested.<sup>15</sup> Nevertheless, crystallization behavior of APCs has not been fully investigated so far.

Recently, we are interested in crystallization of APCs, aiming to better understand the crystal structure and morphology, which have a major impact on the processability and product properties of the materials. Here, we report a unique phase transition of poly(octamethylene carbonate) (POMC), the eighth member (*m* = 8) of APC family, which is highly reminiscent of Brill transition of nylons.<sup>16–20</sup> Using various techniques, we intend to elucidate the mechanism of this transition which cannot be observed in other APCs so far. Our investigations can also help to reveal the fundamentals of Brill transition.

The sample of POMC studied possesses a number-average MW of 36 kg/mol, of which the synthesis and molecular characterization are described in the Supporting Information (SI). The melting temperature (*T*<sub>m</sub>) of POMC is ~68 °C, detected by differential scanning calorimetry (DSC). With a relatively high undercooling, crystallization of POMC was quite fast at room temperature. One-dimensional (1D) wide-angle X-

Received: January 21, 2015

Accepted: February 20, 2015

Published: February 23, 2015

ray diffraction (WAXD) experiment revealed that the crystallized sample rendered two strong diffractions peaked at  $2\theta$  angles of  $20.45^\circ$  and  $23.14^\circ$ , respectively, corresponding to the  $d$ -spacings of 0.43 and 0.38 nm. At higher crystallization temperatures ( $T_c$ s), POMC crystallized slowly. At  $T_c = 50^\circ\text{C}$ , the crystallization required more than 4 h to be completed (Figures S2 and S3 in SI). Interestingly, we found that crystallization of POMC at high  $T_c$ s resulted in a different structure exhibiting a major diffraction located at  $2\theta$  of  $21.91^\circ$  ( $d$ -spacing of 0.41 nm). For convenience, we denote the two crystalline structures observed at around room temperature and around  $50^\circ\text{C}$  the  $\alpha$  and  $\beta$  form, respectively.

To reveal the relationship between the  $\alpha$  and  $\beta$  form of POMC, we employed thermal 1D WAXD to follow in situ the structure evolution upon cooling and subsequent heating (Figure 1, the sample preparation protocol for the WAXD

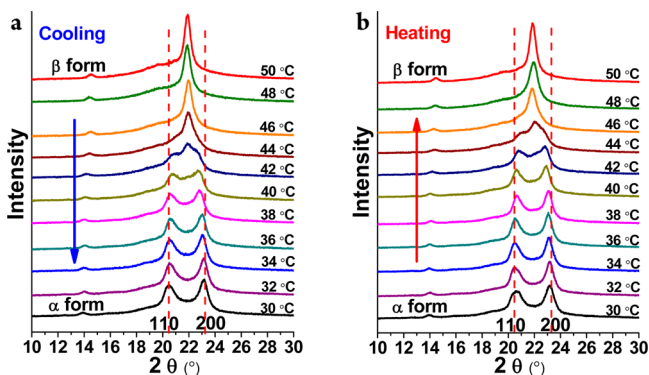
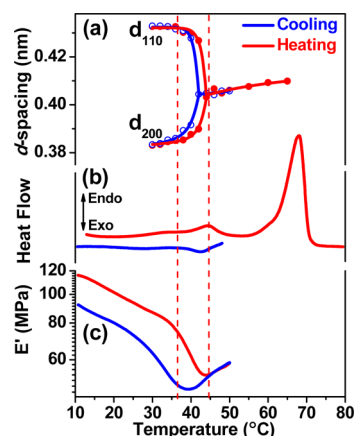


**Figure 1.** Thermal 1D WAXD patterns of POMC measured during (a) cooling from 50 to  $30^\circ\text{C}$  and (b) subsequent heating from 30 to  $50^\circ\text{C}$  ( $\lambda = 1.54 \text{ \AA}$ ).

and other measurements can be found in Figure S4). During cooling of the sample, which was fully crystallized at  $50^\circ\text{C}$  (Figure 1a), the diffraction at  $2\theta$  of  $21.91^\circ$ , the characteristic of  $\beta$  form, is reduced significantly in intensity when the temperature is cooled to  $42^\circ\text{C}$ . Meanwhile, two new peaks appear on both sides of the  $\beta$  form diffraction. Upon further cooling, they become stronger and continuously shift toward opposite directions. At  $30^\circ\text{C}$ , the two peaks are located at  $2\theta$  of  $20.45^\circ$  and  $23.14^\circ$ , respectively. This observation indicates a transition from  $\beta$  to  $\alpha$  form. Figure 1b presents the 1D WAXD profiles recorded during heating from 30 to  $50^\circ\text{C}$ . When the temperature crosses over  $42^\circ\text{C}$ , the  $\alpha$  form diffraction disappears, and that of the  $\beta$  form resets, manifesting the  $\alpha$ -to- $\beta$  transition.

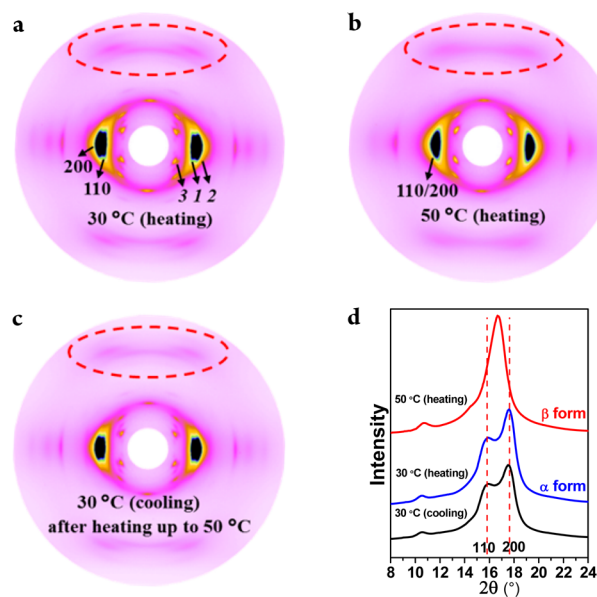
The phenomenon shown in Figure 1 is very similar to that of Brill transition of nylons. Many members of the nylon family demonstrate a reversible transition featuring two diffraction peaks converging into one with increasing temperature,<sup>17–19,21</sup> which was first found by Brill in 1942.<sup>16</sup> In Figure 2a, we plot the  $d$ -spacings of high angle diffractions of  $\alpha$  and  $\beta$  form of POMC as functions of temperature, describing quantitatively the reversibility of  $\alpha$ - $\beta$  transition of POMC. Similar to that found in nylons,<sup>17</sup> a slight hysteresis of the transition temperature is observed between the cooling and heating process. In addition, the transition temperature depended on the initial  $T_c$  applied (Figure S5), which is also observed in nylons.<sup>17</sup>

Figure 2b depicts the DSC thermograms of POMC. After the sample was crystallized into  $\beta$  form at  $50^\circ\text{C}$ , an exothermic



**Figure 2.** Temperature dependence of various experimental data of POMC. The sample used was crystallized at  $T_c = 50^\circ\text{C}$ . (a) Variation of  $d$ -spacings ( $d_{110}$  and  $d_{200}$ ) on cooling from 50 to  $30^\circ\text{C}$  and on subsequent heating to  $65^\circ\text{C}$ . (b) DSC cooling and heating traces recorded on cooling and on subsequent heating. (c) The dynamic Young's modulus ( $E'$ ) on heating and subsequent cooling.

peak around  $42^\circ\text{C}$  is detected upon cooling. During heating, we observe an endotherm peaked at a temperature slightly higher than  $42^\circ\text{C}$ , which is followed by a major melting process beginning at above  $55^\circ\text{C}$ . This result indicates that the  $\alpha$ - $\beta$  transition of POMC is a first-order transition.<sup>22</sup> With a small amount of latent heat, this transition may not invoke a dramatic change of chain packing. To analyze the crystal structures of  $\alpha$  and  $\beta$  form, we performed two-dimensional (2D) WAXD measurements using the oriented sample prepared by uniaxially stretching the crystallized POMC at ambient condition. Figure 3a–c shows the 2D WAXD patterns recorded at 30, 50, and  $30^\circ\text{C}$  (after a heating–cooling cycle), respectively, with the stretching direction along the meridian. The 1D intensity profiles obtained from integration of the 2D



**Figure 3.** 2D WAXD patterns of POMC taken at (a)  $30^\circ\text{C}$ , (b)  $50^\circ\text{C}$  (upon heating), and (c)  $30^\circ\text{C}$  (upon subsequent cooling). (d) 1D integration results of the 2D WAXD patterns shown in (a), (b), and (c). The wavelength of synchrotron X-ray radiation is  $\lambda = 1.24 \text{ \AA}$ . The sample stretching direction is along the meridian.

WAXD patterns are plotted in Figure 3d, consistent with the 1D WAXD results (Figure 1). Therefore, the oriented sample shares the same  $\alpha$ - $\beta$  transition with the powder POMC.

The 2D WAXD experiments confirm that uniaxial stretching can produce the sample with high degree of orientation. At 30 °C, a series of diffraction arcs appear on the equator, with the two strongest ones (1 and 2, indexed in Figure 3a) corresponding to the  $d$ -spacings of 0.43 and 0.38 nm. In the quadrants, a sharp diffraction with the  $d$ -spacing of 0.66 nm (3 in Figure 3a) is observed. Assigning 1 and 2 the (110) and (200) diffraction, respectively, and 3 the (002) diffraction, we can obtain a monoclinic unit cell for the  $\alpha$  form with  $a = 0.77$  nm,  $b = 1.01$  nm,  $c$  (chain axis) = 2.52 nm, and  $\alpha = 31.5^\circ$ . All the diffractions observed in the 2D WAXD pattern can thus be well indexed, of which the results are summarized in Table S1 (the detailed analysis of the crystal structures of POMC will be published with other APCs). Compared to that recorded at 30 °C (Figure 3a,c), the 2D WAXD pattern at 50 °C (Figure 3b) looks quite similar, with the chain orientation maintaining perfectly along the meridian. The most obvious change is that the 1 and 2 merge together on the equator. On the other hand, the diffraction spot 3 moves slightly to a higher  $2\theta$  angle. Note that less diffractions can be detected at 50 °C than at 30 °C, resulting in more difficulty in crystal structure determination. Tentatively, we assume again the diffraction 3 to be (002) and those on the equator to be ( $hk0$ ). As a result, the unit cell of  $\beta$  form, which is also monoclinic, possesses  $a = 0.81$  nm,  $b = 0.89$  nm,  $c$  (chain axis) = 2.42 nm, and  $\alpha = 31.9^\circ$ . The crystallographic data of  $\beta$  form are listed in Table S2.

For both the  $\alpha$  and  $\beta$  form, the monoclinic unit cell contains four repeating units and two chains. According to the chemical structure of POMC, it is considered that the dipole-dipole interaction given by carbonate groups is critical for the chain packing in crystals. The adjacent carbonate groups in a same chain should orientate in opposite directions and can interact effectively with that of neighboring chains, which are antiparallel, through the dipole-dipole interaction. A sort of "sheet" structure may thus be formed (schematic draw is shown in Figure 4, upper panel), which is somewhat similar to the hydrogen-bonded sheet in nylons. In this context, it seems understandable that the  $\alpha$ - $\beta$  transition of POMC can share some common feature with Brill transition of nylons.

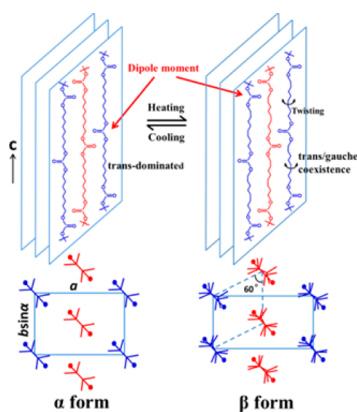


**Figure 4.** Schematic illustration of possible chain packing scheme of POMC in the  $\alpha$  and  $\beta$  form. Upper panel: The assumed "sheet" structure formed due to intermolecular dipole-dipole interaction. Lower panel: The projection of the lattices of  $\alpha$  and  $\beta$  form along the chain direction.

The mechanism of Brill transition remains controversial.<sup>17,18,23–25</sup> One reason for this is that the crystal structure of nylons at above the Brill transition temperature, which can be rather high (e.g., close to 200 °C), is not yet well resolved. It is considered that the conformational change of methylenes in nylons with temperature can be the main origin of Brill transition.<sup>17,21,26–31</sup> Employing solid state NMR and MD simulation, English et al. have found that the methylene groups of nylon-6,6 exhibit large amplitude motions above the Brill transition temperature, but the hydrogen-bonded sheets are maintained until the melting of nylon-6,6.<sup>26,27</sup> Tashiro et al. have studied the Brill transition of nylon-10,10 by using Fourier transform infrared spectroscopy (FT-IR)<sup>21,29</sup> and MD simulation.<sup>30</sup> The trans-dominated conformation of methylenes at low temperatures is observed to change into the trans/gauche coexistence when the temperature becomes higher than the Brill transition temperature. Furthermore, they analyzed the WAXD fiber patterns of nylon-10,10.<sup>31</sup> The diffraction patterns corresponding to the zigzag conformation of methylenes become diffuse after the Brill transition, consistent with the FT-IR results. However, the repeating period of nylon-10,10 formed by the intermolecular hydrogen bonds is still remained in the high temperature phase.

As mentioned above, the comparison between the 2D WAXD patterns of POMC at 30 and 50 °C reveals that the crystal structures at below and above the  $\alpha$ - $\beta$  transition temperature should have the chain packing schemes similar to a large extent. Analogous to that of nylons, the  $\alpha$ - $\beta$  transition of POMC is presumably also largely caused by the conformational change of methylenes. In Figure 3a,c, the diffractions of the trans-dominated conformation of methylenes (denoted by the dashed ellipses in Figure 3a,c) are clear for the  $\alpha$  form. At 50 °C (Figure 3b), they become diffuse after the transition, suggesting that the  $\beta$  form has the methylenes more disordered. This observation is very similar to that found in nylon-10,10.<sup>31</sup>

The conformational change of methylenes of POMC can be well demonstrated by FT-IR experiments, of which the result is shown in Figure 5. The absorption bands in the frequency range of 1440–1500  $\text{cm}^{-1}$  is assigned to the  $\text{CH}_2$  bending mode. In particular, the bands at 1480 and 1469  $\text{cm}^{-1}$  are associated with the trans- and gauche-dominated conformation, respectively.<sup>32–34</sup> During cooling the absorbance at around 1480  $\text{cm}^{-1}$  increases (Figure 5a), while a reversed variation can be observed during heating (Figure 5b). Figure 5c plots the intensity ratio of the band at 1480  $\text{cm}^{-1}$  to that at 1469  $\text{cm}^{-1}$  ( $I_{1480}/I_{1469}$ ) versus temperature. Assuming that the two corresponding vibration modes have the absorption coefficients nearly identical, the increase of  $I_{1480}/I_{1469}$  suggests that the population of trans-dominated methylene sequences increases with lowering temperature. Moreover, the rise of  $I_{1480}/I_{1469}$  speeds up at around 40 °C during cooling, in accordance with the process of  $\alpha$ - $\beta$  transition detected by WAXD and DSC.

The trans-gauche conformational change of the methylene sequences will affect the molecular packing. A straightforward anticipation is that with more gauche conformation the  $c$  axis of  $\beta$  form shall be shorter compared with that of  $\alpha$  form. According to the unit cell parameters deduced from the 2D WAXD results, it can be estimated that when the  $\alpha$  form transformed into the  $\beta$  form the  $c$  axis contracts about 4%, much larger than the 0.18% thermal contraction of polyethylene.<sup>35</sup> Itoh has reported that the molecular chains of nylon-6, -6,6, and -6,10 contract 2.2, 3.7, and 3.9% during Brill

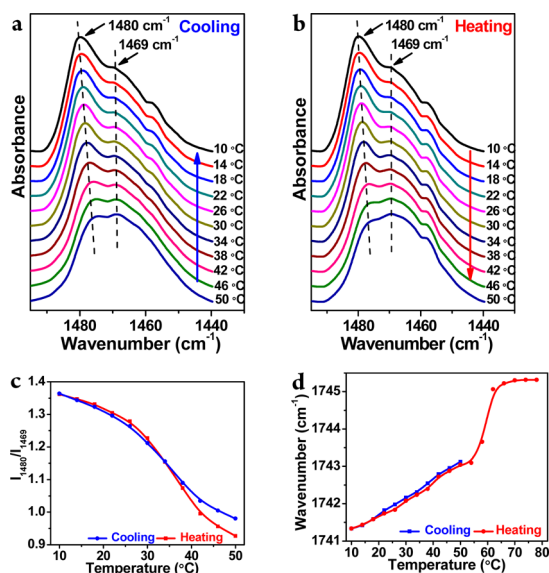


**Figure 5.** (a, b) FT-IR spectra of POMC in the range of 1440–1500  $\text{cm}^{-1}$  obtained from cooling and subsequent heating process, respectively. (c) The intensity ratio of the band at 1480  $\text{cm}^{-1}$  to that at 1469  $\text{cm}^{-1}$  ( $I_{1480}/I_{1469}$ ) and (d) the band wavenumber of carbonyl stretching as functions of temperature. Before FT-IR experiments, the sample was fully crystallized at  $T_c = 50$   $^{\circ}\text{C}$ .

transition, respectively.<sup>24</sup> Our observation is close to these values.

Another consequence of the conformation change of methylene parts is the variation of  $a$  and  $b$  parameters. As shown above, compared with the  $\alpha$  form, the  $\beta$  form of POMC possesses a larger  $a$  but a smaller  $b$ , leading to the  $d$ -spacings of (110) and (200) almost identical (i.e., 0.41 nm). In this case, when viewing along the  $c$  axis, we can observe that the POMC chains in the  $\beta$  form are placed on a pseudohexagonal lattice, which is different from that in the  $\alpha$  form (see the lower panel, Figure 4). This implies that while the methylene sequences become more disordered the carbonate groups may not register as well as that in the  $\alpha$  form. The dipole–dipole interaction between the carbonate groups should be weakened upon heating, but it still intends to keep the ordered chain packing in the  $\beta$  form. Figure 5d depicts the wavenumber of carbonyl stretching ( $\nu_{\text{CO}}$ ) of POMC changing with temperature (the FT-IR spectra are presented in Figure S6). During the  $\alpha$ – $\beta$  transition, the value of  $\nu_{\text{CO}}$  slightly increases with increasing temperature, which may be associated with the weakening of dipole–dipole interaction. When the sample started to melt at above 55  $^{\circ}\text{C}$ , a jump of  $\nu_{\text{CO}}$  is observed, suggesting that the carbonyl groups enter a completely new environment where the dipole–dipole interaction in the crystal is destroyed. This result supports that the mechanism of  $\alpha$ – $\beta$  transition of POMC is mainly the trans–gauche conformational change of methylene sequences. Moreover, loosening the dipole–dipole interaction allows that chains can “jump/rotate” between (110) and (200) in the  $\beta$  form.

It is interesting that POMC exhibits its  $\alpha$ – $\beta$  transition very similar to Brill transition of nylons. In POMC crystals, the carbonate groups provide the dipole–dipole interaction between neighboring chains, much weaker than the hydrogen bonding of nylons which even cannot be completely destroyed at above  $T_m$ .<sup>36</sup> As a result, the  $\alpha$ – $\beta$  transition (or “Brill

transition”) temperature and  $T_m$  of POMC are much lower than that of nylons.

It is well-known that Brill transition is widespread in the nylon family.<sup>19,20,24,29</sup> However, in our study of APCs ( $m = 3$ –10) with similar MW, only POMC, that is, APC-8 ( $m = 8$ ) has been found to possess the “Brill transition” so far (see Figure S7). The exact reason to account for this is unclear at this moment. It may reflect the delicate balance between the methylene segment mobility and the weak dipole–dipole interaction. It is worth mentioning that poly(hexamethylene dithiocarbonate) (PHMDC,  $[-(\text{CH}_2)_6\text{-S-CO-S-}]_n$ ) reported by Berti et al. renders a reversible crystal–crystal transition at around 80  $^{\circ}\text{C}$ .<sup>37</sup> WAXD result of the transition of PHMDC also looks like that of Brill transition. PHMDC and POMC are comparable. Between the two adjacent carbonyl groups, the effective lengths of  $-\text{S}(\text{CH}_2)_6\text{-S-}$  and  $-(\text{CH}_2)_8-$  are similar. Since the electronegativity of the sulfur atom is lower than that of oxygen, the strength of the dipole–dipole interaction between PHMDC chains should be stronger than that in POMC. Consequently, PHMDC possesses higher “Brill transition” temperature and  $T_m$ .

It can be expected that “Brill transition” will affect the mechanical properties of POMC. In this report, some preliminary results based on dynamic mechanical analysis (DMA) are shown in Figure 2c. When heating the fully crystallized sample from 10  $^{\circ}\text{C}$ , the storage modulus ( $E'$ ) decreases slowly at the beginning. A sharp decrease of  $E'$  is observed in the temperature range from 30 to 44  $^{\circ}\text{C}$ , followed by an increase of  $E'$ . The  $E'$  reaches a minimum at the temperature of 44  $^{\circ}\text{C}$ . Therefore, the process of methylene conformation changing from trans-dominated to trans/gauche coexistence makes the sample softer. The minimum  $E'$  is 53.6 MPa, only a half of that measured at 10  $^{\circ}\text{C}$ . Upon cooling the sample, the  $E'$  decreases first and then increases, with a minimum observed at around 40  $^{\circ}\text{C}$ . Currently, more investigation on the mechanical properties of POMC, which depend on the crystal structure and morphology, is undergoing in our lab.

In summary, we find a reversible crystal–crystal transition, namely,  $\alpha$ – $\beta$  transition of POMC by using different techniques. In many aspects, the  $\alpha$ – $\beta$  transition of POMC looks highly similar to Brill transition of nylons. The crystalline structures of the  $\alpha$  and  $\beta$  forms can be analyzed based on 2D WAXD, both of which are monoclinic. Our FT-IR results indicate that the transition is mainly caused by the conformational change of the methylene sequence from trans-dominated at low temperatures to trans/gauche coexistence at high temperatures; in addition to that, the dipole–dipole interaction between the carbonyl groups becomes weaker. This physical picture agrees with that for nylon’s Brill transition proposed by English, Tashiro et al. In APC family, we only observe that POMC possesses the “Brill transition” at this moment. To better understand the crystallization behavior and the structure–property relationship of the green materials of APC, more investigation is required.

## ■ ASSOCIATED CONTENT

### Supporting Information

Synthesis and characterization of POMC, detailed experimental procedures, and additional experimental data. This material is available free of charge via the Internet at <http://pubs.acs.org>.

## ■ AUTHOR INFORMATION

## Corresponding Authors

\*E-mail: liucy@iccas.ac.cn.

\*E-mail: eqchen@pku.edu.cn.

## Notes

The authors declare no competing financial interest.

## ■ ACKNOWLEDGMENTS

This work is supported by National Natural Science Foundation of China (Grant Nos. 21174153, 51273002, and 21304069). The synchrotron 2D WAXS experiment was supported by Shanghai Synchrotron Radiation Facility (SSRF), China.

## ■ REFERENCES

- (1) Chandra, R.; Rustgi, R. *Prog. Polym. Sci.* **1998**, *23*, 1273–1335.
- (2) Raquez, J. M.; Habibi, Y.; Murariu, M.; Dubois, P. *Prog. Polym. Sci.* **2013**, *38*, 1504–1542.
- (3) Rhim, J. W.; Park, H. M.; Ha, C. S. *Prog. Polym. Sci.* **2013**, *38*, 1629–1652.
- (4) Miller, S. A. *ACS Macro Lett.* **2013**, *2*, 550–554.
- (5) Feng, J.; Zhuo, R. X.; Zhang, X. Z. *Prog. Polym. Sci.* **2012**, *37*, 211–236.
- (6) Park, J. H.; Jeon, J. Y.; Lee, J. J.; Jang, Y.; Varghese, J. K.; Lee, B. Y. *Macromolecules* **2013**, *46*, 3301–3308.
- (7) Liu, C.; Jiang, Z.; Decatur, J.; Xie, W.; Gross, R. A. *Macromolecules* **2011**, *44*, 1471–1479.
- (8) Zhu, W. X.; Li, C. C.; Zhang, D.; Guan, G. H.; Xiao, Y. N.; Zheng, L. C. *Polym. Degrad. Stab.* **2012**, *97*, 1589–1595.
- (9) Mespouille, L.; Coulembier, O.; Kawalec, M.; P. Dove, A.; Dubois, P. *Prog. Polym. Sci.* **2014**, *39*, 1144–1164.
- (10) Su, W.; Feng, J.; Wang, H. F.; Zhang, X. Z.; Zhuo, R. X. *Polymer* **2010**, *51*, 1010–1015.
- (11) Zhu, W. X.; Huang, X.; Li, C. C.; Xiao, Y. N.; Zhang, D.; Guan, G. H. *Polym. Int.* **2011**, *60*, 1060–1067.
- (12) Zhao, T. P.; Ning, W.; Zhu, W. X.; Ren, X. K.; Chen, E. Q.; Li, C. C.; Liu, C. Y. Aliphatic polycarbonates: The odd-even effect of crystallization properties caused by the chain length. 2015, Manuscript in preparation.
- (13) Ning, W.; Zhu, W. X.; Zhang, B. Q.; Li, C. C.; Liu, C. Y.; Wang, D. J. *Chin. J. Polym. Sci.* **2012**, *30*, 343–349.
- (14) Takahashi, Y.; Kojima, Y. *Macromolecules* **2003**, *36*, 5139–5143.
- (15) Masubuchi, T.; Sakai, M.; Kojio, K.; Furukawa, M.; Aoyagi, T. *e-J. Soft Mater.* **2007**, *3*, 55–63.
- (16) Brill, R. J. *Prakt. Chem.* **1942**, *161*, 49–64.
- (17) Ramesh, C.; Keller, A.; Eltink, S. J. E. A. *Polymer* **1994**, *35*, 2483–2487.
- (18) Radusch, H. J.; Stolp, M.; Androsch, R. *Polymer* **1994**, *35*, 3568–3571.
- (19) Jones, N. A.; Atkins, E. D. T.; Hill, M. J. *Macromolecules* **2000**, *33*, 2642–2650.
- (20) Jones, N. A.; Cooper, S. J.; Atkins, E. D. T.; Hill, M. J.; Franco, L. J. *Polym. Sci., Polym. Phys.* **1997**, *35*, 675–688.
- (21) Yoshioka, Y.; Tashiro, K.; Ramesh, C. *Polymer* **2003**, *44*, 6407–6417.
- (22) Cheng, S. Z. D.; Keller, A. *Annu. Rev. Mater. Sci.* **1998**, *28*, 533–562.
- (23) Brill, R. *Makromol. Chem.* **1956**, *28/29*, 294.
- (24) Itoh, T. *J. Appl. Phys.* **1976**, *15*, 2295–2306.
- (25) Xenopoulos, A.; Wunderlich, B. *Colloid Polym. Sci.* **1991**, *269*, 375–391.
- (26) Hirschinger, J.; Miura, H.; Gardner, K. H.; English, A. D. *Macromolecules* **1990**, *23*, 2153–2169.
- (27) Wendoloski, J. J.; Gardner, K. H.; Hirschinger, J.; Miura, H.; English, A. D. *Science* **1990**, *247*, 431–436.
- (28) Murthy, N. S.; Curran, S. A.; Aharoni, S. M.; Minor, H. *Macromolecules* **1991**, *24*, 3215–3220.
- (29) Yoshioka, Y.; Tashiro, K. *Polymer* **2003**, *44*, 7007–7019.
- (30) Tashiro, K.; Yoshioka, Y. *Polymer* **2004**, *45*, 4337–4348.
- (31) Tashiro, K.; Yoshioka, Y. *Polymer* **2004**, *45*, 6349–6355.
- (32) Painter, P. C.; Coleman, M. M.; Koenig, J. L. *The Theory of Vibrational Spectroscopy and Its Application to Polymeric Materials*; John Wiley & Sons: New York, 1982; Chapter 15.
- (33) Zheng, R. Q.; Chen, E. Q.; Cheng, S. Z. D.; Xie, F.; Yan, D.; He, T.; Percec, V.; Chu, P.; Ungar, G. *Macromolecules* **2000**, *33*, 5159–5168.
- (34) Zhu, X. Q.; Liu, J. H.; Liu, Y. X.; Chen, E. Q. *Polymer* **2008**, *49*, 3103–3110.
- (35) Kobayashi, Y.; Keller, A. *Polymer* **1970**, *11*, 114–117.
- (36) Kawabata, J.; Matsuba, G.; Nishida, K.; Inoue, R.; Kanaya, T. *J. Appl. Polym. Sci.* **2011**, *122*, 1913–1920.
- (37) Berti, C.; Celli, A.; Marchese, P.; Marianucci, E.; Marega, C.; Causin, V.; Marigo, A. *Polymer* **2007**, *48*, 174–182.